ELSEVIER

Journal of Nuclear Materials 271&272 (1999) 200–204

journal of nuclear materials

High-resolution electron microscopy of γ-TiAl irradiated with 15 keV heliu ions at room temperature

Minghui Song *, Kazuo Furuya, Tatsuhiko Tanabe, Tetsuji Noda

National Research Institute for Metals, 3-13 Sakura, Tsukuba 305-0003, Japan

Abstract

γ-TiAl intermetallic alloy was irradiated with 15 keV He^+ to a dose of 8.6×10^{20} ions m^{-2} (4.4 dpa) in a high-voltage transmission electron microscope (HVTEM) at room temperature, and the evolution of irradiation defects was observed during and after irradiation with HVTEM and high-resolution transmission electron microscopy (HRTEM). Induced defect clusters in γ-TiAl became visible with HVTEM to an irradiation dose of 4.7×10^{19} ions m^{-2} (2.4×10^{-1}dpa). They are mainly planar defects and have a character of domain structures with the edges parallel to {1 1 1) of the matrix and several nanometers in size. Cavities (He bubbles) with irregular shapes were observed in γ-TiAl after He^+ irradiation of 5.7×10^{20} ions m^{-2} (2.9 dpa). Post-irradiation annealing at 673 K for 1800 s enhanced the growth of the domain structure. The analysis of HRTEM images and selected area diffraction (SAD) patterns suggests the formation of rotated domain (RD) which has the same structure as the matrix but in orientations rotating 90° to the matrix. The mechanism of formation of the RD in γ-TiAl crystals is discussed.

1. Introduction

The loss of ductility of the first wall structures due to the helium generated by (n, α) reaction with fusion neutrons is considered to be one of the important problems in the development of fusion materials. Austenitic stainless steels, currently considered as structural materials, generally show severe degradation of mechanical properties when containing several appm He [1,2]. Intermetallic TiAl alloys are being used in airplanes and spaceships manufacturing because of their large strength-to-weight ratio and good resistance in temperature variation conditions [3]. These materials are considered as prospective candidate first wall materials for fusion reactor and some research has been carried out [4].

Several papers have been published on the He^+ and electron irradiation of TiAl alloys [5–8]. Dislocation loops and He bubbles were observed to be formed in γ-TiAl when the materials were irradiated with high energy He ions at temperature of several hundred degree centigrade. The ordered characteristics of intermetallic TiAl alloys was, especially, shown to limit the microstructural evolution under irradiation [6]. However, little is known on the detail of the structures of defect clusters and He bubbles in γ-TiAl irradiated by relatively low energy He ions at low temperature.

The present paper concentrates on a high-resolution transmission electron microscopy (HRTEM) study of the irradiation-induced defects in γ-TiAl intermetallic alloy irradiated by 15 keV He ions in a JEM-ARM1000 high-voltage TEM (HVTEM) operating at 1 MV at room temperature. The characteristics of irradiation defects in γ-TiAl alloy and the effect of post-irradiation annealing are discussed.

2. Experimental

The γ-TiAl alloy with a composition of 49 at.% Ti to 51 at.% Al was manufactured from a skull-melted ingot followed by high temperature extrusion. The block was annealed at 1523 K for 25 h in order to obtain a single γ-phase. Disks, 3 mm in diameter and 0.2 mm thick, were

* Corresponding author. Tel.: +81-298 59 5053; fax: +81-298 59 5054; e-mail: msong@nrim.go.jp

0022-3115/99/$ – see front matter
PII: S0022-3115(98)00706-5

fabricated with mechanical cutting, punching out and polishing. Then the disks were annealed at 1273 K for 1 h to relieve possible strain introduced during mechanical preparation process. The thin foil specimens were electropolished by a twin jet technique in a solution of 10% perchloric acid and 90% ethanol at about 255 K.

He^+ irradiation was carried out in a system consisting of a 1000 keV HVTEM (JEM-ARM1000), a 200 keV and a 30 keV ion implanters at room temperature. The ions were introduced into the specimen in the HVTEM, so that the specimen can be in situ observed when it is irradiated by ions [9]. The accelerating energy of He^+ was 15 keV and the incident angle of the ion beam is 45°. The stopping range and straggling of 15 keV He^+ calculated by TRIM code [10] are about 130 and 55 nm for TiAl, which are appropriate depths in the specimens for a 1000 keV HVTEM observation. The electron beam was switched off during He^+ irradiation in order to eliminate the damages by electron irradiation. The size of ion beam was measured to be 2 mm in diameter. The dose rate and the maximum dose of He^+ were 7.9×10^{16} ions m^{-2} s^{-1} (4.0×10^{-4} dpa s^{-1}) and 8.6×10^{20} ions m^{-2} (4.4 dpa), respectively. Post-irradiation annealing of γ-TiAl specimens was carried out at 673 K for 0.5 h in a vacuum better than 2.0×10^{-6} Pa.

3. Results and discussion

A series of TEM micrographs of γ-TiAl at lower magnification in diffraction contrast (DIFC) mode of TEM observation during He^+ irradiation at a flux of 7.9×10^{16} ions m^{-2} s^{-1} at room temperature is shown in Fig. 1, with the time varying from 0 to 120 min. Since the electron beam of the HVTEM was switched off during the irradiation, it is not possible to observe directly the growth or shrinkage of a defect during the irradiation, but the morphology changes in Fig. 1 is considered as a result of He^+ irradiation. Unclear dot-like defect clusters became visible with TEM after 10 min irradiation of 4.7×10^{19} ions m^{-2}. The density of the defects increased with the irradiation time but the size of the defects did not increase after irradiation up to 60 min. A selected area diffraction pattern (SAD) of the specimen before irradiation (Fig. 1(e)) shows that the specimen is in a single phase of γ-TiAl.

Fig. 2 shows the micrographs of the defect clusters at high magnifications in DIFC mode (Fig. 2(a)) and HRTEM mode (Fig. 2(b)), respectively. The dot-like defects in the γ-TiAl alloy are accompanied by planar defects along one particular {1 1 1} plane as indicated by arrows in Fig. 2(a). It is important to point out, however, that the planar defects are not dislocation loops, which are typical irradiation defects in Al [9], but domain regions with two boundaries parallel to one of {1 1 1} planes, as observed in Fig. 2(b). The width and length of the domains range from several nm to about 10 nm. There is not much dark contrast around the domains. The SAD of the region (Fig. 2(c)) shows two strong streaks in ⟨1 1 1] directions that correspond to the domain structure in the matrix. The difference of the lattice contrast in two sides of some boundaries (Fig. 2(b)) suggests the differences in crystal structure between the domain and the matrix.

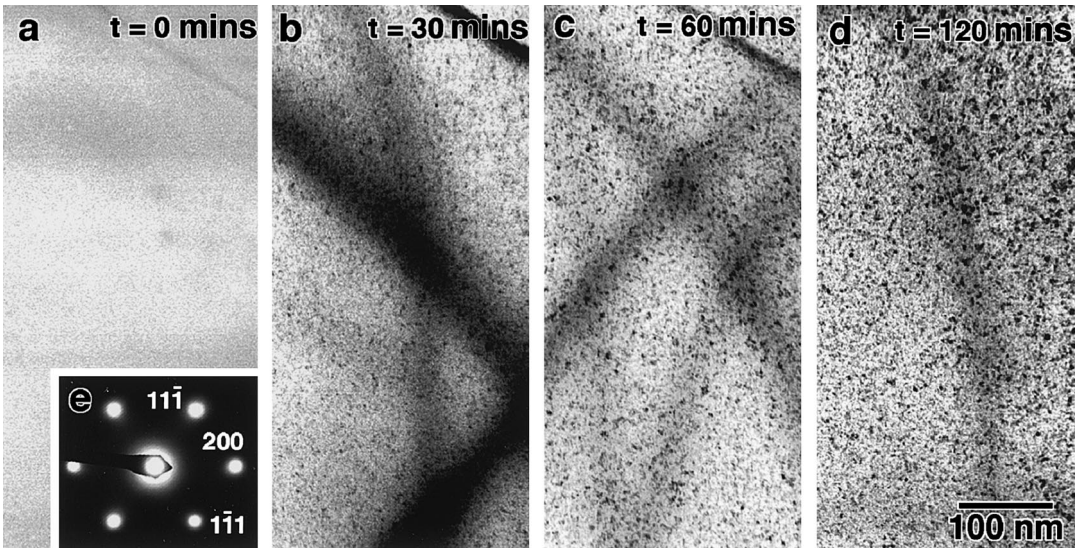

Fig. 1. A series of HVTEM micrographs showing the evolution of defect clusters in γ-TiAl in DIFC mode during 15 keV He^+ irradiation with a flux of 7.9×10^{16} ions m^{-2} s^{-1} (4.0×10^{-4} dpa s^{-1}) at room temperature. (a) 0 min. (b) 30 min. (c) 60 min. (d) 120 min. (e) A selected area diffraction (SAD) pattern.

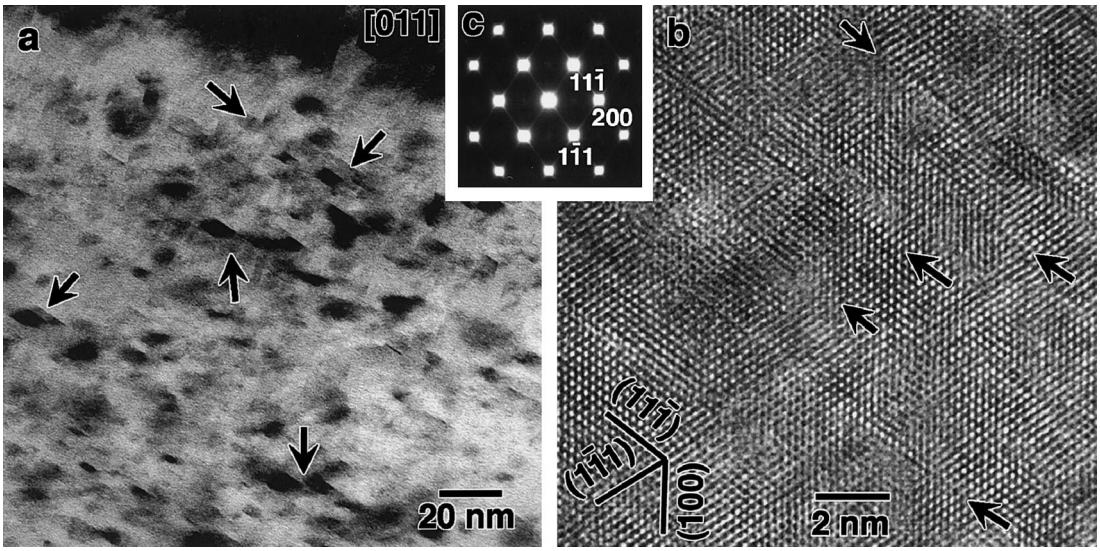

Fig. 2. Irradiation defect clusters in γ-TiAl irradiated by 15 keV He^+ to a dose of 8.6×10^{20} ions m^{-2} (4.4 dpa) at room temperature. (a) A low magnification image in DIFC mode, showing domain-like defects, marked by arrows. (b) A HRTEM image of domain-like defects. (c) An SAD pattern.

Weak extra spots can be observed in the SAD at positions equal to 1/2[2 0 0] (Fig. 2(c)). The extra spots can be explained by the existence of a small portion in another crystal orientation, which has a relation to the matrix of 90° rotation and is noted as rotated domain (RD) [11–13]. When the incident direction of electron beam is chosen to be [0 1 1] along the matrix, that will be [1 1 0] for some of these rotated portions which will produce (0 0 1) superlattice reflection. The image of the domains is clear in DIFC mode (Fig. 2(a)), while that is unclear in HRTEM mode (Fig. 2(b)). Since the domain is small and with interface along {1 1 1) with the matrix, the streaks along ⟨1 1 1] in the SAD were formed. The γ-TiAl has an ordered $L1_0$ structure and its anti-phase boundary (APB) energy has been reported to be high [14]. The APB accompanied by RD can be introduced in γ-TiAl by quenching [11–13]. The present work reveals that the He irradiation can also produce the RD.

Cavities were found in thick region of the irradiated γ-TiAl specimens. Fig. 3 shows a photograph in DIFC mode for the specimen irradiated by He ions to a dose of 5.7×10^{20} ions m^{-2} (2.9 dpa). The cavities, marked by arrows, are seen to be white because the micrograph was taken in underfocus. The shape of the cavities is irregular and its size is in a range of 5–10 nm. Since they were observed in the specimen after He^+ irradiation, it is reasonable to think them as He bubbles. The formation of He-bubbles in γ-TiAl were previously reported after the irradiation by 200 keV He^+ at 773 K [5,7]. The present results shows that the possible migration and aggregation of He atoms in γ-TiAl alloy at room temperature may produce the He-bubbles.

Fig. 4 presents HVTEM micrographs in DIFC and HRTEM mode with SAD pattern for the γ-TiAl specimens irradiated by He^+ to a dose of 8.6×10^{20} ions m^{-2} (4.4 dpa) and subsequently annealed at 673 K for 1800 s. The extra spots become stronger and can be seen more clearly. The streaks in ⟨1 1 1] also become stronger than

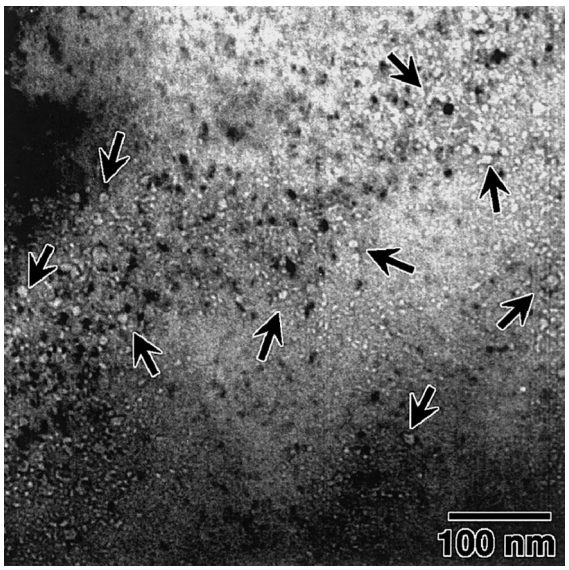

Fig. 3. A HVTEM micrograph of cavities (He-bubbles, marked by arrows) in γ-TiAl formed by 15 keV He^+ to a dose of 5.7×10^{20} ions m^{-2} (2.9 dpa) at room temperature. The size of the cavities ranges up to several nanometers.

that in Fig. 2(c). These facts indicate that the post-irradiation annealing enhanced the nucleation or/and growth of the RD. Fig. 4(a) shows a dark field image using a 200 spot and an extra spot at 1/2[2 0 0]. In addition to the domain structures, weak fringes parallel to (2 0 0) plane can be seen in the figure. Considering the characteristics of $L1_0$ structure of γ-TiAl, an RD formed in matrix has two possible direction relations to the matrix, one is in a relation of rotating 90° on [1 0 0] direction (A type) and another on [0 1 0] direction (B-type). When the matrix is observed in [0 1 1] direction, the direction can be in [1 1 0] or [1 0 1] direction of the two kinds of RDs, respectively. The extra spots in Fig. 4(c) are superlattice reflections of [0 0 1] in A type RDs, so that the fringes observed in Fig. 4(a) are superlattice fringes of the A type RDs. Corresponding to the superlattice fringes in Fig. 4(a), enhancement of lattice fringes is also observed in HRTEM in Fig. 4(b), shown by arrows. The spacing of the enhanced fringes is the same as the lattice parameter of γ-TiAl (0.40 nm). The enhancement is considered to result from the overlapping of (1 0 0) of the matrix and (0 0 1) of an A type RD, since the (0 0 1) is parallel to and has a spacing very close to that of (1 0 0). Since the streaks and extra spots in SAD did not appear for unirradiated specimens with the same heat treatment conditions, it is clear that the radiation induced defect and clusters with He ions and/or the implanted He ions have contribution to the formation of RDs.

It is generally known for the γ-TiAl phase that the ordered arrangement of Ti and Al atoms is stable up to its melting point, so that no disordered f.c.c. phase exists in an equilibrium state at elevated temperature [15], and also, the APB energy is known to be high [14]. When the γ-TiAl phase is kept under irradiation, interstitials and vacancies are considered to migrate preferably on (0 0 1) plane, in which Ti and Al atoms are stacked periodically [5]. But if the irradiated He atoms get associated with the movement of interstitials and vacancies, the interstitials and vacancies may move on other planes, for example, {1 1 1). This movement of atoms and vacancies can be a possible mechanism for the formation of RD in the present work.

A HVTEM operated at 1 MV was used in the present work, typical periods of time for observation before and during ion irradiation were 30 min and several minutes, respectively. Although the irradiation of 1 MeV electron beam at elevated temperature induces defect clusters in TiAl alloys [8], we believe the electron beam irradiation did not influence our results apparently.

4. Conclusions

Effects of 15 keV He^+ irradiation on microstructural evolution in γ-TiAl alloy and the effects of post-irradiation annealing in γ-TiAl alloy were investigated by means of high-resolution electron microscopy. Planar defect clusters with size up to several nanometers became visible after 10 min irradiation corresponding to a dose of 4.7×10^{19} ions m^{-2} (2.4×10^{-1}dpa). The character of the planar defects in γ-TiAl is a domain

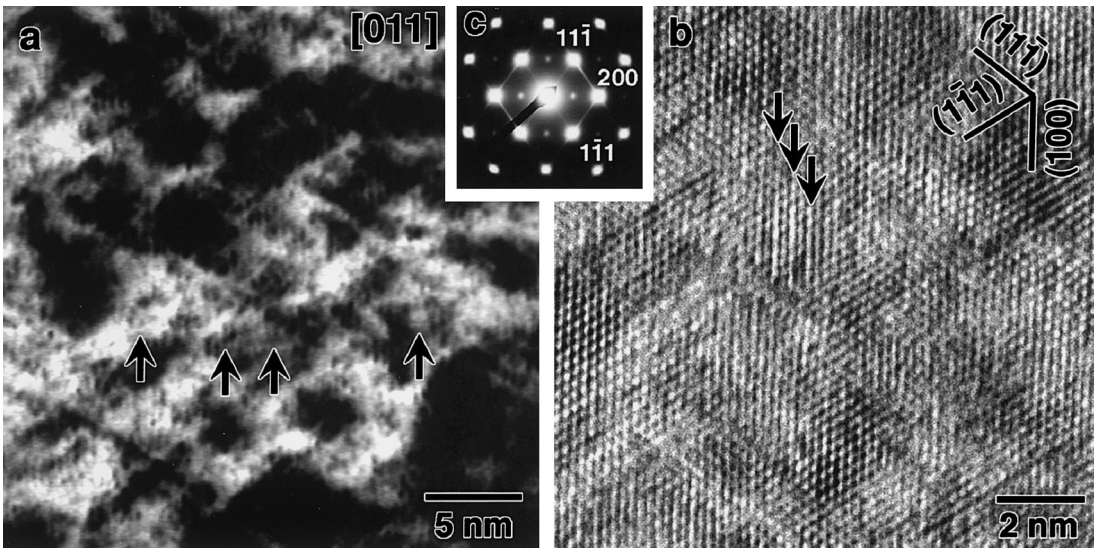

Fig. 4. Irradiation defects in γ-TiAl irradiated by 15 keV He^+ to a dose of 8.6×10^{20} ions m^{-2} at room temperature and subsequently annealed at 673 K for 0.5 h. (a) A dark field image in DIFC mode, showing superlattice fringes of rotated domains (RD) aligned along (1 0 0) plane by arrows. (b) A HRTEM image, showing RDs and enhancement of fringes resulted from overlapping of an RD and matrix crystals indicated by arrows. (c) An SAD pattern.

structure with the edges parallel to {1 1 1) of the matrix, which can be explained as RD. Cavities (He bubbles) with irregular shapes were observed after He^+ irradiation of 5.7×10^{20} ions m^{-2} (2.9 dpa). Post-irradiation annealing of γ-TiAl at 673 K for 0.5 h enhanced the formation of the RD. The formation of the RD should be associated with He^+ irradiation.

References

[1] S.A. Fabritsiev, A.S. Pokrovsky, V.A. Brovko, J. Nucl. Mater. 233–237 (1996) 173.
[2] H. Schroeder, H. Ulmaier, J. Nucl. Mater. 179–181 (1991) 118.
[3] M. Matsuo, ISIJ Int. 31 (1991) 1212.
[4] S. Mori, H. Miura, S. Yamazaki, T. Suzuki, A. Shimizu, Y. Seki, T. Kunugi, S. Nishino, N. Fujisawa, A. Hishinuma, M. Kikuchi, Fusion Technol. 21 (1992) 1744.
[5] K. Nakata, K. Fukai, A. Hishinuma, K. Ameyama, M. Tokizane, J. Nucl. Mater. 202 (1993) 39.
[6] A. Hishinuma, J. Nucl. Mater. 239 (1996) 267.
[7] K. Nakata, K. Fukai, A. Hishinuma, K. Ameyama, J. Nucl. Mater. 240 (1997) 221.
[8] A. Hishinuma, K. Nakata, K. Fukai, K. Ameyama, M. Tokizane, J. Nucl. Mater. 199 (1993) 167.
[9] K. Furuya, M. Piao, N. Ishikawa, T. Saito, Mater. Res. Soc. Symp. Proc. 439 (1997) 331.
[10] J.F. Ziegler, J.P. Biersack, U. Littmark, in: J.F. Ziegler (Ed.), The Stopping and Range of Ions in Solids, Pergamon, New York, 1985.
[11] E. Abe, M. Nakamura, Philos. Mag. Lett. 75 (1997) 65.
[12] M.H. Loretto, Philos. Mag. Lett. 68 (1993) 289.
[13] M.H. Loretto, Philos. Mag. A 71 (1995) 421.
[14] D. Schectman, M.J. Blackburn, H.A. Lipsitt, Metall. Trans. 5 (1974) 1373.
[15] C. McCullough, J.J. Valencia, C.G. Levi, R. Mehrabian, Acta Metall. 37 (1989) 1321.